ADVANCING EARTH AND SPACE SCIENCE

JGR Space Physics

RESEARCH ARTICLE
10.1029/2020JA029072

Key Points:

- The twin episodes of pre-reversal enhancement (PRE) in the post-sunset hours over Tirunelveli linked with under/over shielding electric fields
- The unusual height enhancement at all three ionosonde stations in the dawn sector due to the effect of eastward disturbance dynamo electric field
- Vertical and zonal plasma drifts showed large oscillations but are anti-correlated

Correspondence to:
S. Sripathi,
ssripathi.iig@gmail.com;
sripathi.s@iigm.res.in

Citation:
Singh, R., & Sripathi, S. (2021). The role of storm-time electrodynamics in the dawn and dusk sectors across equatorial and low-latitude ionosphere during December 19–21, 2015. *Journal of Geophysical Research: Space Physics*, *126*, e2020JA029072. https://doi.org/10.1029/2020JA029072

Received 23 DEC 2020
Accepted 28 JUN 2021

The Role of Storm-Time Electrodynamics in the Dawn and Dusk Sectors Across Equatorial and Low-Latitude Ionosphere During December 19–21, 2015

Ram Singh[1,2] and S. Sripathi[1]

[1]Indian Institute of Geomagnetism, Navi Mumbai, India, [2]Vikram Sarabhai Space Centre (VSSC), Space Physics Laboratory, Thiruvananthapuram, India

Abstract We present the distinct responses of the nighttime ionosphere due to an intense and long lasting geomagnetic storm of December 19–21, 2015 using a chain of ionosondes from magnetic equator to anomaly crest region over India. The observations exhibited unique features throughout the night including dawn and dusk sectors. The results showed twin episodes of pre-reversal enhancement (PRE) in dusk sector associated with oscillatory vertical plasma drift due to shielding electric field that produced briefly post-sunset equatorial spread F (ESF) irregularities. Accordingly, relative dominance of interplanetary magnetic field (IMF) and auroral electrojet (AE) related electric field fluctuations in vertical and zonal drifts at different times are investigated throughout the night. Also the application of wavelet/wavelet coherence analysis on interplanetary and geomagnetic conditions and ionospheric data showed distinct relationships. The results showed that vertical drift is in phase with interplanetary electric fields (IEFy) with period of ~30 min at ~18:30 IST (13:00 UT) that drives first PRE whereas ~60 min period in AE which is in phase with vertical drifts drives second PRE at ~20:30 IST (15:00 UT). However, other short term periods in vertical drifts are in phase with IEFy and AE at other times suggesting that both are contributing to the drift variations. The simultaneous upliftment of F layer at all stations producing fresh ESF irregularities in the dawn sector is attributed to the unique electrodynamical response of the Indian low latitude stations to the eastward disturbance dynamo electric fields (DDEFs). These results are also in concomitant with satellite observations and thermospheric ionospheric electrodynamics general circulation model (TIE-GCM) drifts.

Plain Language Summary The electrodynamics at equatorial and low latitude ionosphere is significantly modified during geomagnetic storms due to convection electric fields and auroral thermospheric winds at high latitudes. While signatures of prompt penetration electric fields can be seen instantly in the equatorial ionosphere as undershielding or overshielding electric fields, the thermospheric winds and its associated disturbance electric fields reach the equator with a delay depending upon their propagation speeds. Our observations showed twin episodes of pre-reversal enhancement (PRE) in the dusk sector which is attributed to undershielding and overshielding conditions respectively during an intense geomagnetic storm of December 19–20, 2015. In the midnight to post-midnight, the h'F (km) and drifts have undergone several oscillations with their highest peaks occurring in the dawn sector. The most striking feature is the enhancement in virtual height in the dawn sector and associated drifts during the recovery phase. Further analysis indicates varied impacts of IEFy and AE index on the vertical plasma drift oscillations at short and long periods. In addition, presence of large upward vertical plasma drift and occurrence of fresh plasma irregularities as seen in the dawn sector could be linked to the strong eastward disturbance dynamo (DD) electric field.

1. Introduction

The storm-time electrodynamics of the equatorial and low latitude ionosphere is significantly modified from quiet-time behavior due to additional disturbances caused due to the magnetospheric convection electric fields, substorm related electric fields and outflow of auroral thermospheric winds to mid and low latitudes due to Joule heating at high latitudes (e.g., Kamide & Chian, 2007; Spiro et al., 1988). During geomagnetic storms, the convection electric field of the magnetospheric origin promptly penetrates to the equator as prompt penetration (PP) electric field through propagation of transverse magnetic mode in the

Earth-Ionosphere waveguide (e.g., Kikuchi, 1986) with the eastward and westward polarities during the day and night respectively (e.g., Kikuchi et al., 1996; Sastri, 1988; Spiro et al., 1988). This adds to the existing solar quiet (Sq) electric fields to make equatorial ionospheric electrodynamics very unique. This also either enhances or reduces the existing upward plasma drift in the dusk sector which could ultimately cause Raleigh Taylor (RT) instability to either to grow leading to the generation of equatorial spread-F (ESF) irregularities or their suppression (e.g., Abdu et al., 1981; Fejer et al., 1991). The ESF irregularities are generated in a complex way that encompasses a wide range of scale size of density irregularities. It is believed that the ESF irregularities develop through the RT inter-change instability mechanism acting on the seed perturbations in the density and polarization electric field generated by the gravity waves at the bottomside of the sharply rising post-sunset F layer. The eastward thermospheric zonal wind in the evening hours generates vertical polarization electric field in the F layer that has strong longitudinal gradient across the sunset terminator due to the decay in the E layer conductivity toward the night side. This condition leads to the development of pre-reversal enhancement (PRE; e.g., Abdu et al., 2003; Farley et al., 1986; Fejer et al., 1991; Heelis et al., 1974; Kelley et al., 2014; Rishbeth, 1971). As these irregularities evolve non-linearly to higher altitudes and bifurcate, these irregularities can also be detected instantaneously at lower latitudes and anomaly crest regions. The storm time thermospheric winds, waves and its associated disturbance dynamo (DD) electric fields also influence the equator, however, with a delay depending upon their propagation speeds (e.g., Araki et al., 1985; Blanc & Richmond, 1980; Fejer et al., 1983). The order of this time delay is from few hours to few days after the onset of geomagnetic storm. The zonal component of disturbance dynamo electric fields during daytime is in westward and is opposite to the quiet time ionospheric dynamo electric field which is eastward during daytime, while it is in eastward direction in the night where quiet time zonal electric field is in westward direction (e.g., Blanc & Richmond. 1980). For PP electric field, the imbalance between Region-1 (R1) and Region-2 (R2) field-aligned currents (FACs) and their horizontal closure currents play significant role and may directly be related to the solar wind parameters (e.g., Kelley et al., 1979; Kikuchi et al., 1996; Sastri et al., 1992). In addition, the PP electric fields may also be penetrated under the different phases of magnetic storm due to sudden changes in the polarity of Interplanetary Magnetic Field (IMF Bz; i.e., southward and northward; e.g., Abdu et al., 1998; Astafyeva et el., 2018; Cherniak & Zakharenkova, 2016; Huang et al., 2007; Kikuchi et al., 1996; Liu et al., 2014; Ram Singh & Sripathi, 2017; Ram Singh et al., 2015; Sastri et al., 1992, 2000). As the arrival time and phases of the PP and DD electric fields and winds and waves are distinctly different, it is possible to separate their contributions. But when the geomagnetic storm is prolonged for a long duration, it is difficult to identify these sources properly as all the above mentioned factors will be playing their roles at different times. In addition, Abdu et al. (1998) have suggested that low latitude electrodynamics under geomagnetic storms modifies the vertical polarization electric fields significantly. They surmised that vertical polarization electric field can arise due to combination of the following processes: (a) Hall conduction, (b) neutral wind dynamo and (c) vertical currents arising from divergence of horizontal (zonal) currents. These combinations can cause storm-time fluctuations in both zonal and vertical drifts at equatorial and low latitudes (that is anti-correlated to each other). Also, background neutral density and conductivity play significant roles in deciding how much they impact the equatorial and low latitudes. Also since the quiet time electric fields are modified significantly from time to time, day-to-day and season, it is very difficult to isolate the contributions of quiet time variabilities from storm time variability. It is only possible to estimate individual contributions to a certain extent. Chakrabarty et al. (2008) have investigated a case of geomagnetic storm event in this respect on how to separate the different effects of interplanetary electric fields (IEFy) and substorm generated auroral electrojet (AE) electric fields on pre-mid night time equatorial F layer using airglow and ionosonde measurements. They identified the effects of IEFy and AE index in the equatorial F layer height using the FFT and its phase analysis techniques.

Over the equatorial region, the dawn and dusk sector electrodynamics are very important and play significant role in causing post-sunset and post-midnight equatorial plasma irregularities. As the terminators across dawn and dusk sectors provide sharp density gradients, these sectors are usually conducive for generation of strong polarization electric fields. There are significant similarities in the electrodynamics during dawn and dusk sectors (e.g., Kelley et al., 2014). During the post sunset and pre-sunrise periods, F region vertical plasma drifts are primarily driven by zonal electric field formed as a part of polarization electric field developed due to the thermospheric winds and sharp conductivity gradients in the E-region (e.g., Fejer et al., 1991). The vertical plasma drift due to primary zonal electric field is generally upward in the daytime and downward in the nighttime during magnetically quiet time. Past studies on the vertical/zonal plasma drifts around the sunset and sunrise hours suggest that they are dominated by both E and F region dynamos due to day and night transition (e.g., Farley et al., 1986; Fejer et al., 1999; Prabhakaran Nayar et al., 2009; Rishbeth, 1971; Sekar & Kelley, 1998). Their studies suggested that zonal electric field pushes the F layer to higher altitudes in the presence of a sharply depleting E region conductivity and polarization electric field in the dawn and dusk terminators (e.g., Farley et al., 1986).

Further, it is known that the nocturnal zonal and vertical electric fields over the equatorial region are also significantly affected by the geomagnetic storms and substorms (e.g., Abdu et al., 1998; Kelley et al., 2003; Reddy et al., 1979, 1990; Sastri, 2002). Accordingly, the generation and inhibition of plasma irregularities at equatorial and low latitudes are also significantly affected by geomagnetic storms. While occurrence of equatorial plasma irregularities have been attributed mainly to the RT instability process, low latitude plasma irregularities can be attributed to the mapping of equatorial plasma irregularities and in situ generation of plasma irregularities at the edges of sharp density gradients generated during geomagnetic storms. Reddy et al. (1990) reported the characteristics of disturbed electric fields and showed importance of substorms on the electric fields at low and mid-latitudes. They suggested that the virtual height (h′F) enhancements at five Japanese stations are due to the magnetospheric substorms related to eastward electric field in the morning sector. Kelley et al. (2014) have reported few quiet time observations of sunrise enhancement in the vertical plasma drift using the Communication/Navigation Outage Forecasting System (C/NOFS) satellite. Statistical analysis of quite time results using ROCSAT1 vertical drifts in the dawn sector has showed frequent occurrence of pre-sunrise enhancement during June solstice but least during winter reported (e.g., Zhang et al., 2015, 2016). They suggested that increase of drifts in the dawn sector could be related to differences in the lag time of sunset in the conjugate E regions across the hemispheres. However, our observations as presented in this paper suggest that vertical plasma drift could be enhanced during pre-sunrise hours as well in winter solstice that is linked to an intense geomagnetic storm of December 19–20, 2015. Also our observations show anti-correlation of vertical drifts with zonal drifts that is reported in South America (Abdu et al., 1998). In the present study, an attempt has been made to delineate the effects of IEFy (storm related) and AE (substorm-related) electric field perturbations on equatorial F region zonal and vertical electric fields during December 20, 2015 night when both storm and substorms were present simultaneously. We also try to understand the causes for twin episodes of PRE in the dusk sector and causes for unusual height enhancement in the pre-sunrise hours at an equatorial station at Tirunelveli over India during this third strongest geomagnetic storm of solar cycle-24 namely December 19–21, 2015 where the Dst index reached its peak (minimum) value of −175 nT. The relationships between solar wind and equatorial ionospheric parameters during this magnetic storm have been thoroughly examined here where the vertical (zonal) plasma drift variations during the sunset and pre sunrise hours were having unusual fluctuations/oscillations and anti-correlating each other. While post-sunset electrodynamics during quiet and storm time have been studied through observations and theory, height enhancement during pre-sunrise hours and their causative mechanisms are not well understood during both quiet and disturbed periods. Also we note that though number of studies have been made on the pre-sunrise PRE in the recent past, their studies were mostly related to electrodynamics of quiet times. In addition, we also present results based on thermospheric ionospheric electrodynamics general circulation model (TIE-GCM) to validate our observations and also investigate the model analysis to provide additional insights.

2. Data Sets

The solar wind parameters namely solar wind dynamic pressure, solar wind velocity, interplanetary electric and magnetic fields are obtained from the CDAWeb (http://cdaweb.gsfc.nasa.gov/). The temporal resolution of solar wind parameters is 1 min. The geomagnetic activity indices such as symmetric component of ring current (SYM-H), AE, and Kp indices are obtained from the World Data Center (WDC), Kyoto university. Three Canadian advanced digital ionosondes (CADIs) located at Tirunelveli (8.73°N, 77.70°E; geom 0.34°N), an equatorial station, Hyderabad (17.36°N, 78.47°E; geom 8.76°N), a low latitude station and Allahabad (25.3°N, 81.5°E; geom 16.5°N) which is located in the northern edge of the equatorial ionization anomaly (EIA) crest region in India are analyzed for ionospheric parameters such as h′F, foF2 and Doppler drift. The ionograms are manually scaled for these ionospheric parameters at 10 min time interval over the

Tirunelveli and Hyderabad and 5 min time interval overAllahabad during the quiet and storm periods. Also, the Doppler drift mode of observations at few selected frequencies namely 2–8 MHz at Tirunelveli is operated at 1 min interval in addition to ionogram mode continuously. This provides drift information about zonal, vertical and meridional directions. The strength of equatorial electrojet (EEJ) is measured by the difference of horizontal component of geomagnetic field that is ΔH_{TIR} and ΔH_{ABG} ($\Delta H_{TIR} - \Delta H_{ABG}$) between two pairs of ground-based magnetometers located at equatorial station Tirunelveli (8.73°N, 77.70°E) and off equatorial station at Alibag (18.5°N, 72.9°E) over Indian longitude respectively after correcting for base line in the midnight (e.g., Rastogi & Klobuchar, 1990).

3. Results

3.1. Interplanetary and Geomagnetic Conditions on December 19–21, 2015

An intense geomagnetic storm has occurred during December 19–21, 2015 with the Dst minimum value of ∼−175 nT, when the two earth-directed asymmetrical full-halo Coronal Mass Ejections (CMEs) hit the Earth on December 19 at 15:30 UT. Both asymmetrical full-halo CMEs were observed by SOHO/LASCO C2 coronagraph imageries on December 16. The first CME was observed in C2 imagery beginning on December 16 at 09:24 UT. The second CME associated with a filament eruption was first observed in coronagraph imagery at December 16 at 14:36 UT. Both CMEs were Earth-directed and arrived at Earth later on December 19. The CMEs from December 16 probably merged in the interplanetary medium and impacted the Earth on December 19 at 15:28 UT and produced intense geomagnetic storm. This storm was the third major storm of the solar cycle-24 and also third major storm in 2015.

Figures 1a–1f gives a general overview of interplanetary and geomagnetic conditions during the December 19–21, 2015. It can be seen that how the onset of intense geomagnetic storm takes place at around ∼15:30 UT on December 19 when two asymmetrical full-halo CMEs hit the Earth's magnetosphere and how the magnetospheric conditions were abruptly changed (vertical green line indicates CME hitting time with Earth's magnetosphere on December 19). The solar wind Pressure (Psw) increased abruptly from ∼2 to 20 nPa, solar wind velocity (Vsw) reached from ∼350 to 500 km/sec and Bz component of interplanetary magnetic field showed mostly northward orientation on December 19. Slowly the IMF Bz (Figure 1c) started fluctuating between north and south between 15:30 and 04:00 UT on December 19–20. On December 20, at around 04:30 UT, IMF Bz sharply turned from north to south reached its peak value of −16 nT, and it has prolonged for ∼36 h in the southward direction until 18:00 UT on December 21. When the IMF Bz was fluctuating from north to south, intensification of auroral activities were noticed which is an indication of substorm activity. During the main phase of the magnetic storm, AE index shows an enhancement in its value and the maximum value it reached is ∼18:00 nT on December 20 (Figure 1d). The sharp reduction in SYM-H at ∼04:30 UT marked the starting of main phase. Initially it was moderate geomagnetic storm with the intensity of SYM-H value ∼−88 nT at 08:30 UT and later SYM-H reached its peak (minimum) value of ∼−175 nT at 23:00 UT on December 20 (Figure 1e). Figure 1f shows the temporal variation of EEJ strength on the storm day (blue) along with five International Quiet Days (IQDs) average value (black). On the December 20 around at ∼03:30 UT, EEJ values were fluctuating between ±50 nT and coinciding with the turnings of IMF Bz suggesting the penetration of eastward and westward electric fields from high latitude to equator in the undershielding and overshielding conditions. In Figure, shaded regions are indicative of the signatures of PP and DD electric fields.

3.2. Ionospheric Response as Seen by Chain of Ionosondes at Tirunelveli/Hyderabad/Allahabad

Now in this section, we present ionospheric response during the main and recovery phases of the geomagnetic storm on December 20–21, 2015 as seen by the CADI ionosondes. Figure 2a shows the variation of virtual height (h′F, in km) of F layer in red color during 12:00–12:00 IST (06:30–06:30 UT; IST=UT-5.5) on December 20–21, 2015 along with mean variation of h′F at every 15 min on entire month of December 2015 shown in blue color with error bars. The light black color scatter plots show the variations of h′F during the month of December and bold black color lines representing the onset and duration of spread-F irregularities. The orange color shaded regions show the time of twin PRE in the post-sunset and height enhancement in the morning hours (morning hours PRE). Figure 2b depicts the height-time-frequency

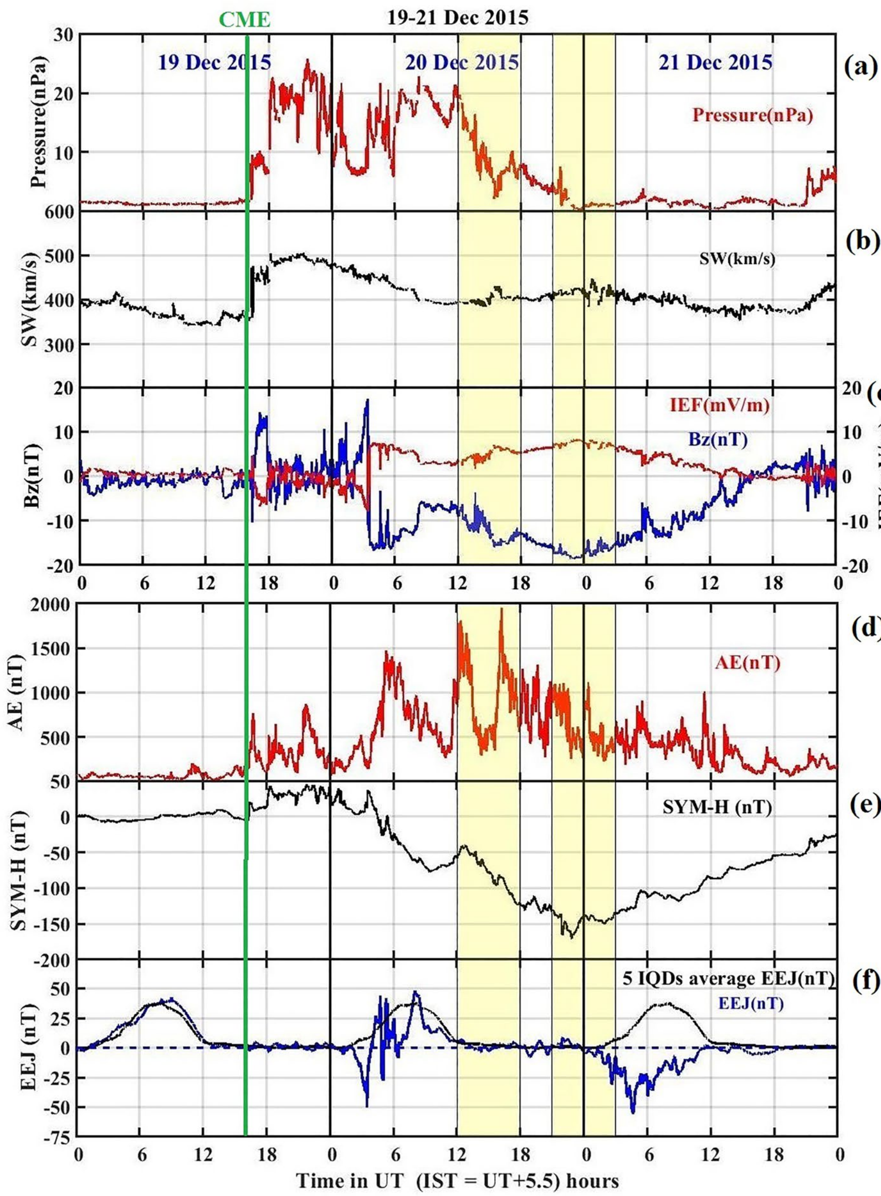

Figure 1. Solar and geomagnetic activity indices namely (a) solar wind pressure, (b) solar wind velocity (SW), (c) Interplanetary magnetic field (IMF Bz) (blue) &, Interplanetary electric field (IEF) (red), (d) auroral electrojet index (AE), (e) symmetric component of ring current (SYM-H), and (f) equatorial electrojet (EEJ) strength (blue), five international quiet days (IQDs) mean value of EEJ (black) for the period of December 19–21, 2015. The shaded vertical boxes during the 12:00–18:00 IST and 21:00–03:00 IST indicate the presence of disturbances.

(HTF) variation at different frequencies, ranging from 4.0 to 9.0 MHz. This Figure 2b also shows nicely the rise of height in the post-sunset and post-midnight with smaller oscillations throughout night. From both Figures 3a and 3b it can be seen that the height rise at twin times is ~400 and 375 km respectively (see point 1 and 2) with a dip at ~20:30 IST is observed between ~18:00 and 21:00 IST. This dip is reaching its value of ~270 km. Thereafter, h′F shows minor oscillatory behavior in its value during the remaining night time between 21:00 and 03:00 IST (shown by points 2, 3, and 4). However, during the pre-sunrise hours at ~05:30 IST, a conspicuous enhancement is observed in virtual height where the height reached its maximum altitude of ~600 km with ~50 m/sec vertical drift (vertical drift shown in Figure 5a) which is higher than the post-sunset drift. This produced ESF irregularities for a brief period in the ionosonde observations. Usually, the post sunset height is higher. But this much rise in the dawn sector in the virtual height was not seen

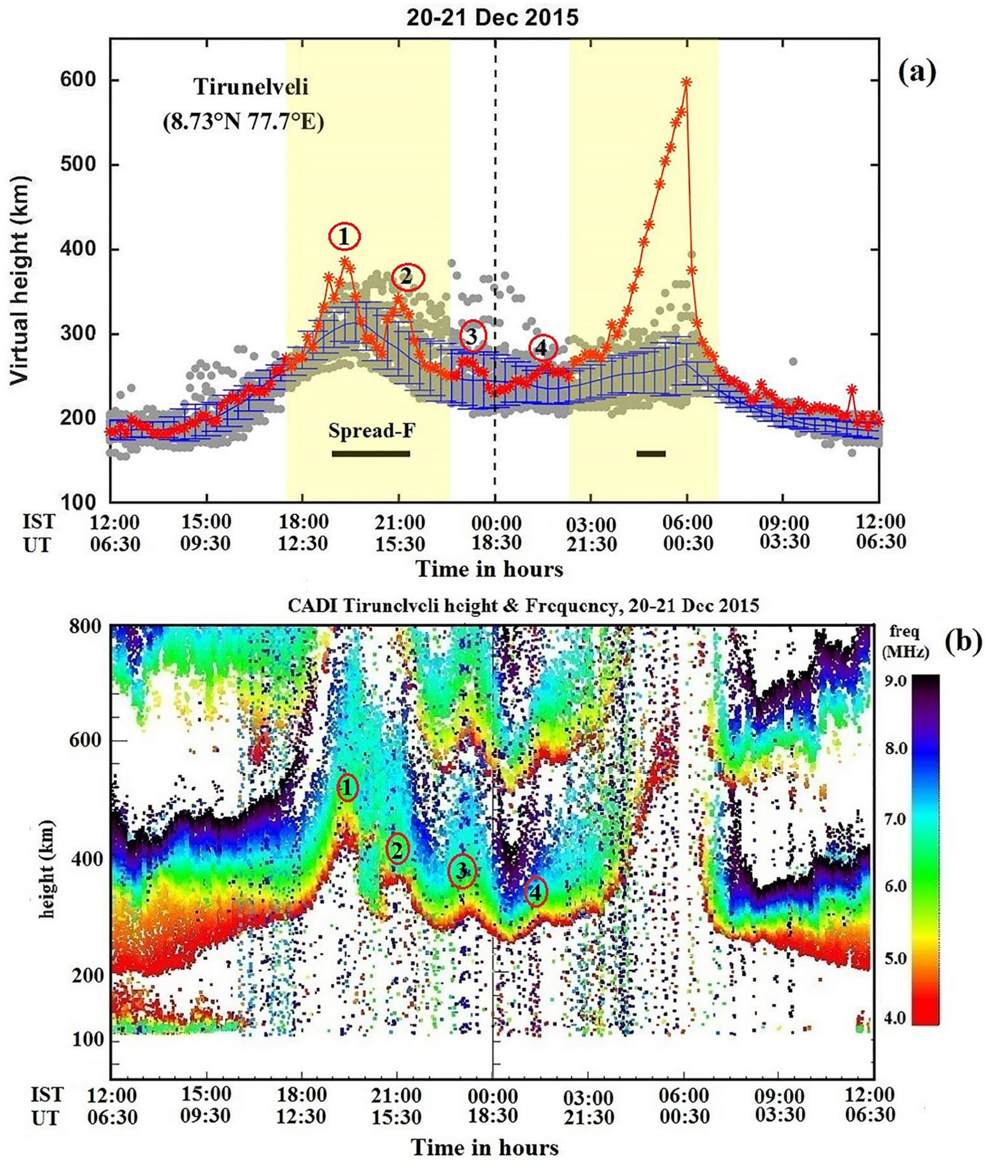

Figure 2. Temporal variation of nighttime ionospheric parameters namely (a) Virtual height (h′F) in km (red) along with mean of h′F on entire month of December 2015 (light black color scatter plots show h′F and blue color line with error bars shows the mean value of h′F) at Tirunelveli. The shaded vertical boxes during the 17:00–23:00 IST and 01:00–07:00 IST indicate the evening and pre-sunrise hour height enhancement. (b) The variation of Range-Time-Frequency (RTF) at frequencies between 4 and 9 MHz on December 20–21, 2015.

during any other storm time and any other quiet days during the entire month. We could also examine all the days during the whole year in 2015 to see whether such height rise were observed but concluded that none of the day's height could rose to this much in altitude in the dawn sector except on this day that is on December 21, 2015. So, this day appears to be interesting case to study.

Figures 3a–3f shows the temporal variation of (left) virtual height and (right) foF2 (MHz) at three ionosonde stations namely Tirunelveli, Hyderabad and Allahabad during 11:30–11:30 IST (06:00–06:00 UT; IST = UT + 5.5 h) on December 20–21, 2015 along with mean variation of h′F as obtained at every 15 min on five international Quiet Days (IQDs) which is shown in blue color error bars, bold black color lines representing the onset and durations of spread-F irregularities and pink color shaded regions show simultaneous height enhancement at all the three stations during evening and morning hours. In December 2015, five IQDs are 03, 04, 18, 28, and 30. From the Figure it can be seen that ionospheric height is enhanced

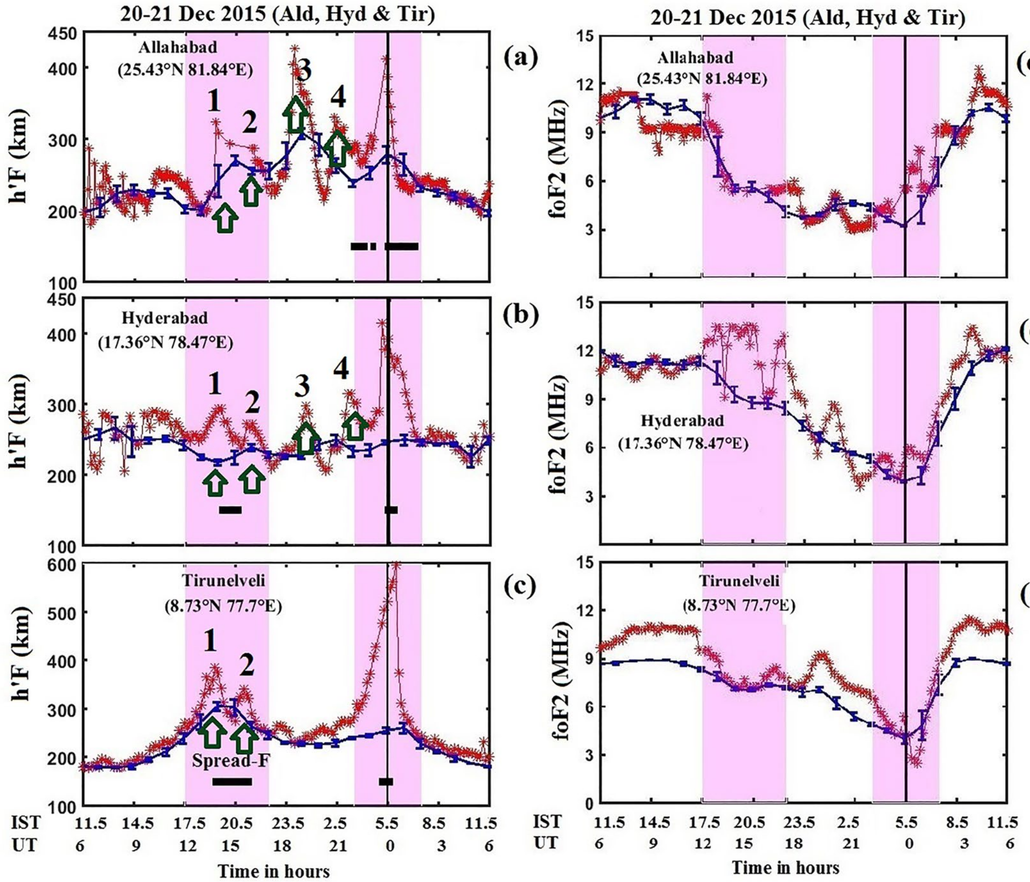

Figure 3. Shows temporal variation of (left) ionospheric height (virtual height (h′F)) in km and (right) foF2 (MHz) at Tirunelveli (bottom), Hyderabad (middle) and Allahabad (top) over Indian region [(a) h′F in km (red) and five international quiet days (IQDs) mean value (blue) of h′F at Allahabad, (b) h′F in km (red) at Hyderabad, and (c) h′F in km (red) at Tirunelveli]. The shaded vertical boxes during the 17:00–22:00 IST and 01:00–07:00 IST indicate the height enhancements during evening and pre-sunrise hours.

simultaneously at all three stations under undershielding and overshielding electric field conditions at ∼13:00 and 15:00 UT (18:30 and 20:30 IST) in the pre-midnight hours as indicated by the peaks 1 and 2. At the same time, foF2 also shows density variations at all the stations. However, the amplitude of density oscillations was significantly higher at Hyderabad. Also it can be seen that ionospheric heights were showing oscillatory behavior throughout the night at all the three latitudes that is, associated with substorm activity at times. However, these oscillations were dominant mainly at Allahabad followed by Hyderabad and Tirunelveli. During the local midnight hours that is at around 17:30 (23:30 IST) and 20:00 (01:30 IST) UT, the first ionospheric height enhancement over Allahabad (indicated by the peak 3 and 4 in Figure 3a) can be seen and after ∼1 h delay, such enhancement can be seen over Hyderabad at ∼18:30 and 21:00 UT (indicated by the peak 3 and 4 in Figure 3b). At the same time, foF2 also shows density enhancements at all the stations simultaneously. At the dawn sector, Tirunelveli showed lowest density as compared to other two stations where density increased. But at Tirunelveli, Hyderabad and Allahabad, significant height oscillations were noticed at dawn sector. During the Pre-sunrise hours, ionospheric height is almost simultaneously enhanced over all the three stations at ∼05:30 IST. The height and density oscillations were having good correlation at all the three stations. It also can be seen that spread F at Allahabad is observed mainly in the dawn sector whereas at Tirunelveli and Hyderabad, it is seen at both dawn and dusk sectors. This suggest that these spread F structures at Allahabad could be independent of equatorial type spread F. Rather it can be of local/mid-latitude type structures which are excited due to storm induced height oscillations. In order to investigate further on these structures, we scaled the ionogram at isoheights for all the three stations. Figures 4a–4c shows the temporal variation of isoheights during 12:30–06:30 UT (18:00–12:00 IST)

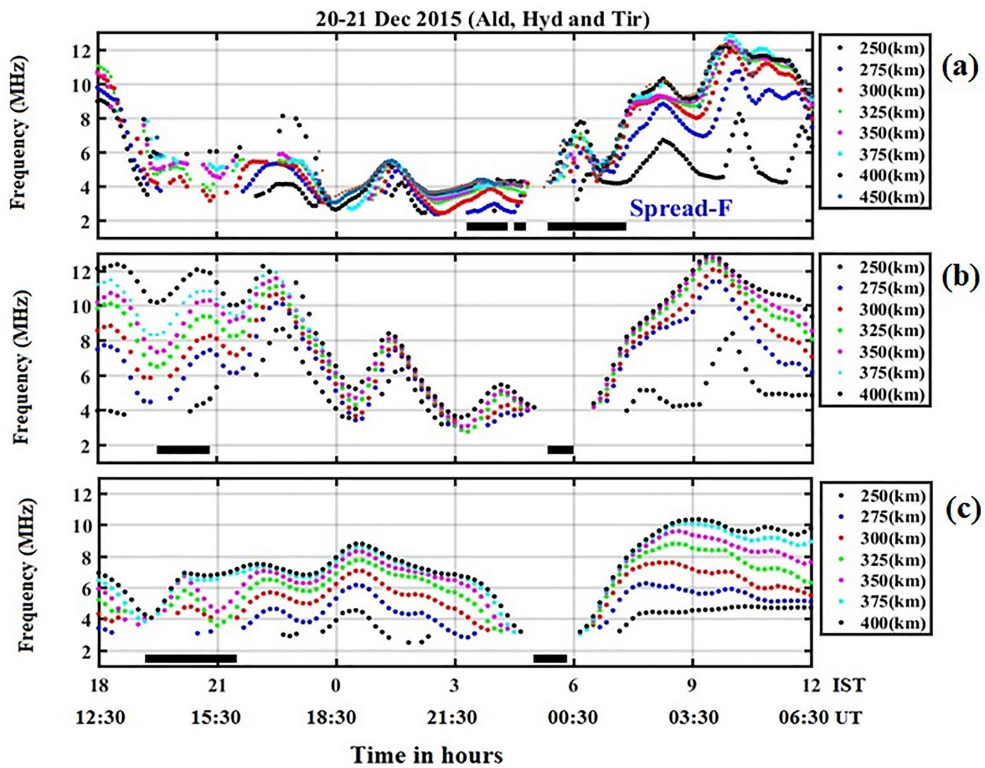

Figure 4. Shows the temporal variation of nighttime F region density variations at isoheights at Tirunelveli (bottom), Hyderabad (middle) and Allahabad (top) stations respectively on December 20–21, 2015. The spread F duration is shown as black patch at the bottom of the figure.

at Tirunelveli (bottom), Hyderabad (middle) and Allahabad (top) as scaled at 250–450 km at 25 km resolution. The different colors indicate different heights. Here spread F duration is denoted at the bottom of the figure. It can be seen from the figure that there is a large variation in the density at all the stations. These density oscillations appear to be highly coherent at all the stations. To understand more about the sources for these density variations, we further compare equatorial vertical drifts with AE and IMF Bz variations in the next figure.

3.3. Equatorial Plasma Vertical/Zonal Drifts and Their Variations

Figures 5a–5d shows the diurnal variation of vertical and zonal plasma drifts along with AE and IMF Bz variations from 11:30 IST on December 20 to 11:30 IST on December 21, 2015. In Figure 5a we show the vertical plasma drift (red) as obtained from Doppler drift mode of CADI ionosonde at 4 MHz frequency for the better trend and continuity along with dh′F/dt drift (red) as calculated by the rate of change of F layer virtual height (h′F) which is again from the CADI ionosonde. The zonal plasma drift (blue) which is also obtained from ionosonde is shown in next subplot (b). Figure 5c shows AE indices (blue) along with smoothed AE variation (red) for better comparison as obtained by Savitzky–Golay (SG) algorithm (Savitzky & Golay, 1964). The advantage of SG algorithm is its ability to suppress the noise with less distortion of original signal. The bottom side panel in Figure shows IMF Bz variations. From this Figure, we can see that slow variations in both vertical and zonal plasma drifts shows similar variations as that of AE Index but anti-correlated each other at times. The shaded regions show drift variations from evening to next day morning between ∼17:30 and 07:30 IST. The shaded region between ∼17:30 and 22:30 IST show the first peak of PRE vertical drift enhancement at ∼18:30 IST where vertical drift is enhanced upto ∼30 m/sec upward (eastward electric field) and turned downward (westward electric field) at ∼19:00 IST reached upto ∼45 m/sec and again turned upward at ∼21:00 IST. Similarly, the zonal drift shows weak west ward drifts in the evening hours with several oscillations afterward but they are anti-correlated with vertical

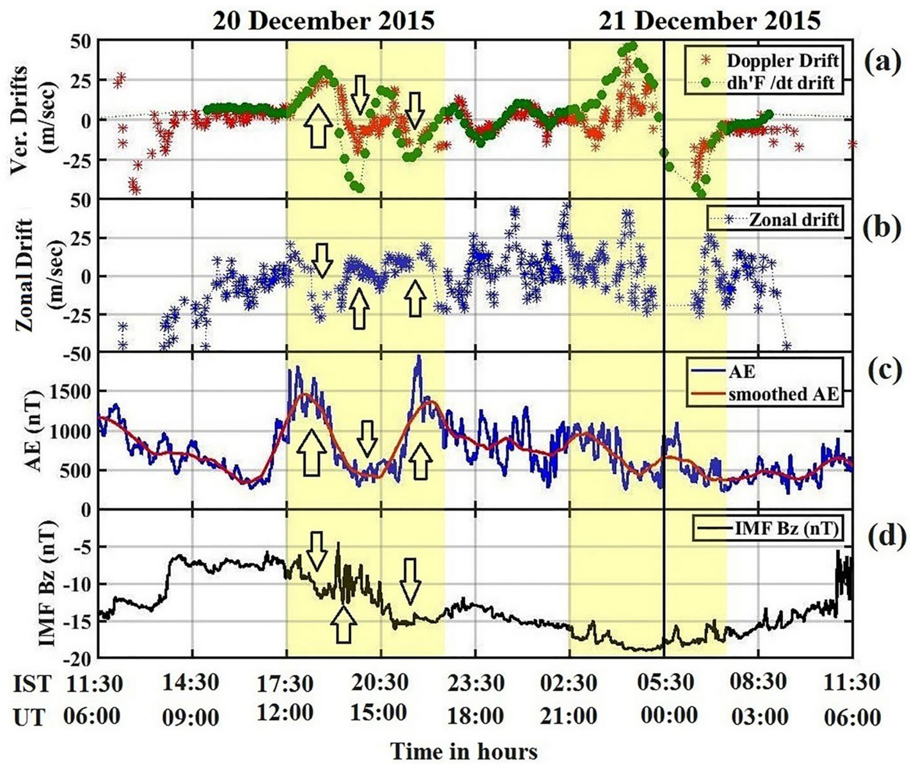

Figure 5. (a) Shows temporal variation of nighttime F-region vertical Doppler drift (red) at 4 MHz frequency and dh′F/dt (green) in m/sec, (b) zonal plasma drift (m/sec) over Tirunelveli as obtained from Canadian advanced digital ionosonde (CADI) ionosonde along with (c) corresponding AE (nT) index and smoothed auroral electrojet (AE) index (red color) and (d) corresponding variations in interplanetary magnetic field (IMF) Bz (nT) on December 20–21, 2015. The shaded regions indicate evening and pre sunrise hours of pre-reversal enhancement (PRE). The upward and downward arrows show the variations in in phase and out of phase of drift with interplanetary electric fields (IEFy) and AE indices.

drifts oscillations at times as discussed previously. It can be noticed that whenever IMF Bz turns south and northward (representing by the downward an upward arrows in the Figures), the vertical plasma drifts are also correspondingly either going upward or downward at the same time. Thereafter the vertical drift was seen fluctuating with minor oscillations throughout the night until 03:00 IST. At ∼03:30 IST, vertical drift started increasing and reached its maximum value of upto ∼50 m/sec at ∼05:30 IST (pre sunrise hours) but suddenly turns downward and reached ∼−50 m/sec (∼07:30 IST). The similar type of fluctuations were also observed in the AE index; however, their phases were either shifted positively or negatively. During the evening hours (shaded region) enhancement and reduction are well correlated to IMF Bz, which is the cause of undershielding and overshielding electric field. Interesting point to be noted from the Figure 5 is that whenever there is a change is noticed in either AE or IMF Bz in the pre-midnight sector, corresponding change is observed in the vertical and zonal drifts. It can be seen that the rising phase of AE index causes eastward electric field (upward drifts) but westward zonal drifts penetration, while descending phase causes westward electric field (downward drifts) but eastward zonal drift penetration at magnetic equator. The drifts are such that zonal and vertical drifts are anti-correlated to each other. Such anti-correlated equatorial plasma oscillations have been reported in Brazilian sector in the past. However, no such correlation is seen in the dawn sector. It is possible that the dawn sector rise in the virtual height could be due to eastward disturbance dynamo electric fields associated with peculiar electrodynamics around dawn sector. Also please recall that the observation of EEJ strength as shown in Figure 1 suggests that EEJ variations were also seen in the post-midnight when vertical drift shows its oscillatory behavior throughout the night. The variations in the EEJ strength suggest that they could be related to the equatorial plasma drifts on this night as E region conductivity is negligibly small in the post-midnight.

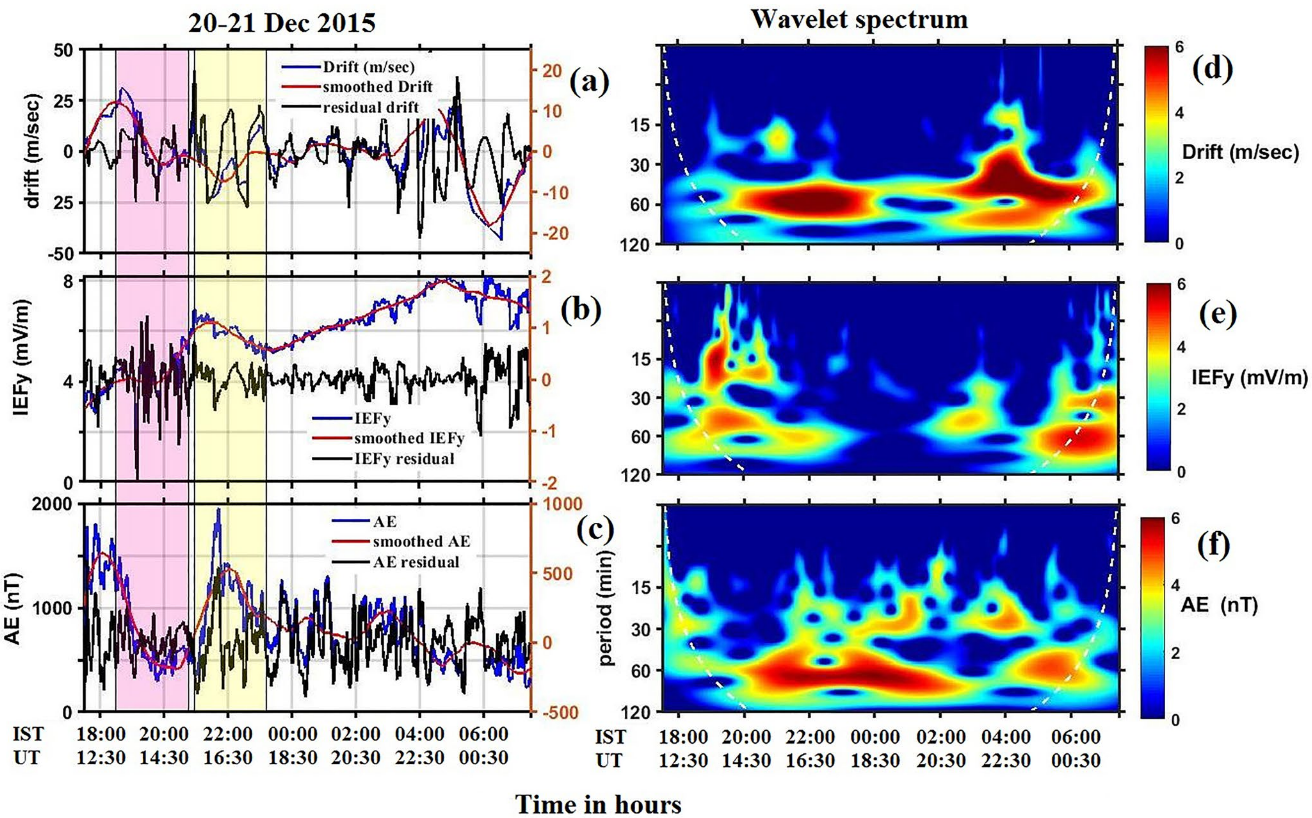

Figure 6. (a–c) the blue color lines show the variations in vertical drift, solar wind velocity, and interplanetary electric fields (IEFy) between 17:30 and 07.30 IST on December 20–21, 2015, red color lines represent smoothed value of respective parameter and black color lines represent residual value. The shaded vertical boxes indicate the in phase and out of phase variations of residual value of drift, IEFy and auroral electrojet (AE), and (d–f) (left) Morlet wavelet spectrum analysis during the same period between 17:30 and 07.30 IST of respective parameters.

3.4. Wavelet/Cross-Wavelet Analysis on Solar, Geomagnetic and Ionospheric Parameters

As we have seen above that it is possible to have storm time PP electric fields and substorm related electric field perturbations in the equatorial drifts when both storm and substorms are present simultaneously. Similarly, it is possible to have the role of DD electric fields or disturbance winds or TIDs or combination of these forces simultaneously when the storm is prolonged for several hours. However, it may be noted that it is possible to separate them to certain extent through application wavelets/cross-wavelets and its coherence analysis.

Accordingly, to understand their signatures, we performed further analysis using the Morlet wavelet analysis (Torrence & Compo, 1998). Figures 6a–6f shows the temporal variation of drift and IEFy and AE indices (a, b, and c) along with a smoothed curve based on the SG algorithm (red), residual curve (black) and their wavelet spectrum (d, e, and f) on their residuals between 17:30 and 07:30 IST on December 20–21, 2015. From the Figure (in shaded region and orange) it can be seen clearly that residual of vertical drift believed to be correlated with residuals of both AE and IEFy at times (showed in the pink color shaded region). The wavelet spectrum analysis shows smaller and larger dominant periods with period of ~20 and 50–70 min in drift, IEFy and AE indices. The vertical drift shows dominant periods at ~20 min at ~18:30,21:00 and 04:00 IST, but 50–70 min between 20:00 and 00:00 IST, thereafter ~40 min between ~03:00 and 07:00 IST ~30–70 min (Figure 6d), IEFy shows ~15–70 min between ~18:00–22:00 IST and ~40–70 min between 02:00 and 07:30 IST (Figure 6e), and AE index shows the ~40–70 min between ~20:00–02:00 and 04:30–07:00 IST (Figure 6f).

From the above figures, we note that it is difficult to identify which factor is playing dominant role using wavelet alone as both were having near similar periods. Accordingly, we examined the cross wavelets and

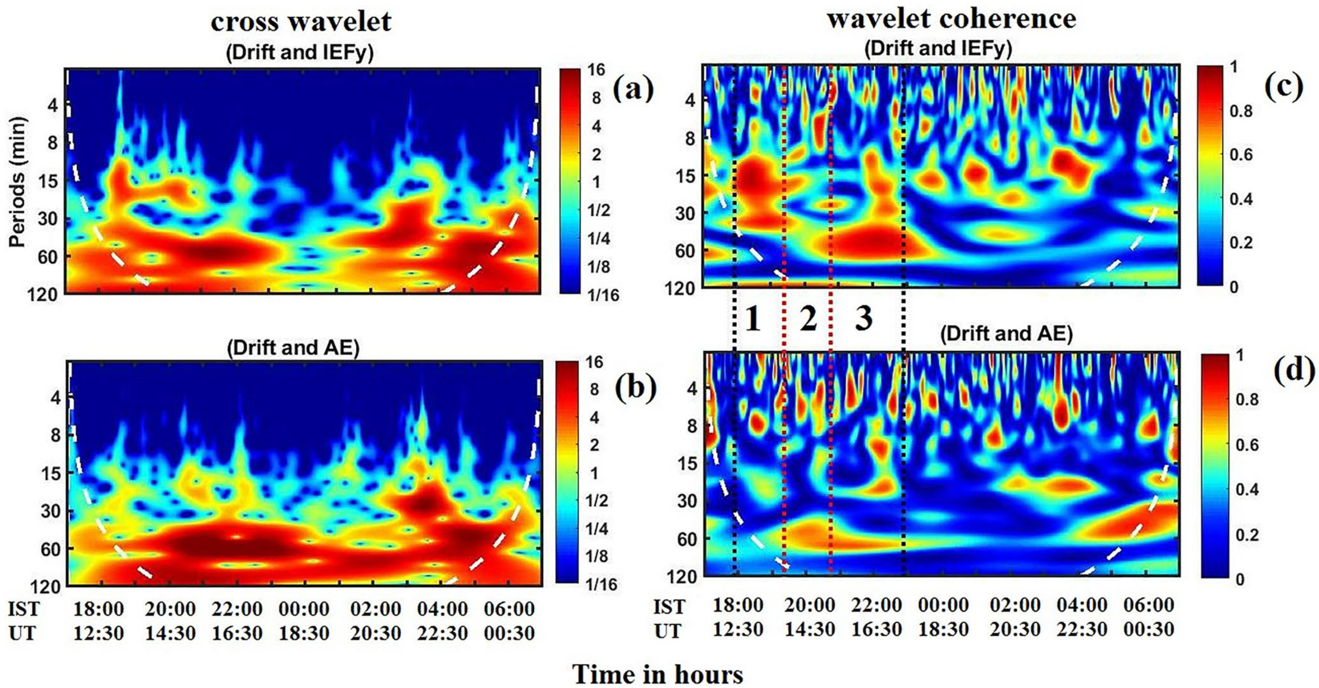

Figure 7. Cross-wavelet (Morlet) analysis between drift (residual) and residual of (a) interplanetary electric fields (IEFy), (b) auroral electrojet (AE) index, and wavelet coherence between drift (residual) and residual of (c) IEFy, and (d) AE index between 17:30 and 07:30 IST on December 20–21, 2015. Region-1 (between black and red vertical lines) shows times when ~30 min period in drift are similar/in phase with IEFy but out of phase with AE, region-2 indicates times when (between two vertical lines) ~60 min period in drift are similar/in phase with AE but out of phase with IEFy, and region-3 represents times when ~20 and 60 min periods are similar/in phase between drift, IEF and AE.

coherence analysis using wavelet coherence (e.g., Marques de Souza et al., 2018). This technique has been widely used in geophysical applications to identify the source region. The cross-wavelet analysis is useful to identify the times when the two parameters such as drifts and IEFy are having same period. But, wavelet coherence between these two parameters can suggest whether they are in phase or out of phase. According to this, their periods could be similar but their coherence may not be similar suggesting that their phase is either advanced or delayed. Figures 7a–7b shows the cross wavelet and wavelet coherence analysis of vertical plasma drift between (a) IEFy and (b) AE index. Figure 7a shows common dominant periods of ~20 min at ~18:00–21:00 IST between drift and electric fields, which are not common with AE index (in Figure 7b). From the Figures 7a and 7b it can be seen clearly that dominant common periods are ~20–70 min between ~20:00 and 23:00 IST and ~20–70 min between 03:00 and 06:00 IST. However, wavelet coherence analysis shows ~15–30 min periods are in same phase between drift and IEFy at ~18:30–20:00 IST. But these periods are out of phase with AE as shown in the region 1 between black and red horizontal lines. Thereafter vertical drift and AE index are having same periods with period of ~60 min at 20:00 IST and out of phase with IEFy as shown in region 2 between two horizontal red lines. The period of ~60 min is same for vertical drift, IEFy and AE indices at ~20:30–23:00 IST and period of ~20 min are also common for them and in same phase (region-3 between two red and black horizontal lines). This analysis suggest that the first peak of PRE is correlated to the fast fluctuations (~20–30 min periods, which are in same phase) in the interplanetary electric field, however the second peak of PRE is associated with combined effect of AE and IEFy (where dominant periods ~60 min are in same phase with AE and IEFy). This can be noticed through wavelet coherence observations. However, interestingly, only AE indices having ~60 min period are showing dominant signature in the wavelet coherence. But as this time falls under recovery phase, there might be disturbance electric fields and winds at play. Accordingly, we believe that during the pre-sunrise hours vertical drift enhancement as seen here could be caused by strong eastward disturbance electric field associated with AE and disturbance dynamo electric field effect in association with some peculiar local dawn sector electrodynamic phenomenon linked with this storm. Accordingly, drifts in the dawn sector could be related to the electric field fluctuations in the auroral latitudes that are causing this sudden enhancement at

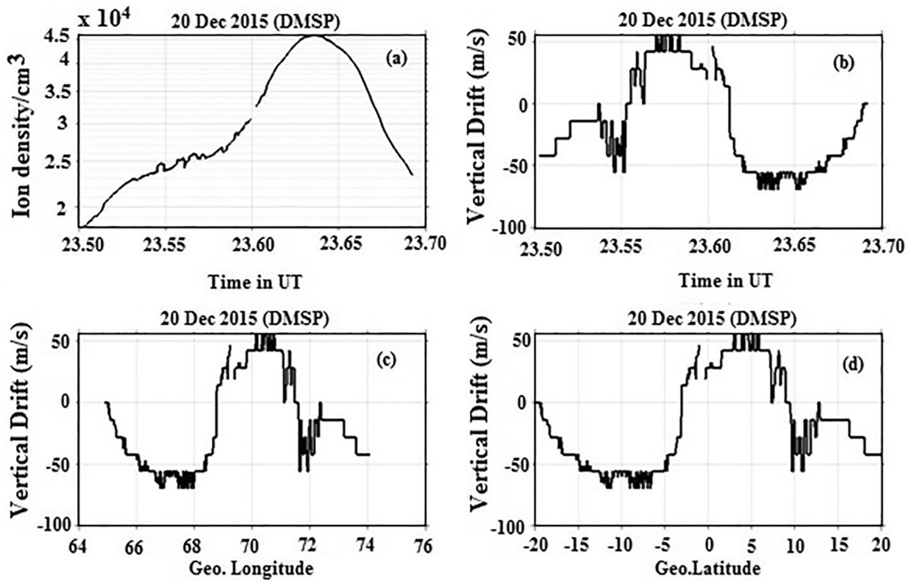

Figure 8. (top) Temporal variation of DMSP satellite measured (a) ion density (cc/cm^3), (b) vertical drifts (m/s); (bottom) (c) Longitude and (d) Latitude variation of these vertical drifts in the dawn sector on December 20, 2015 coincides with Doppler drifts from Canadian advanced digital ionosonde (CADI).

~60 min period which is in coherence. From the above analysis it is found that ~30 min periods are associated with IEFy and ~60 min periods are caused either by AE or by both IEFy and AE.

As CADI drifts in early morning or dawn sector could be contaminated by errors due to non-availability of many reflecting or scattering regions, we examined the ion density and their vertical drifts over Indian sector by DMSP satellite located at the altitude range of ~850 km on December 20, 2015 as shown in Figures 8a–8d. While ion density variations as a function of time is shown in Figure 8a (top; left), vertical drift variations of the ion motion as a function of latitude, longitude and time are shown in Figures 8b–8d. From the figure, it can be seen that vertical drifts as measured by DMSP also shows upward in the dawn sector over Indian sector indicating that ionosonde measured vertical drifts are indeed correct and is not artifact of the measurements. The magnitude of the drifts also matches very well with satellite observations. Also the ion density shows several fluctuations in Figure 8a during the same time suggesting that plasma bubbles were indeed present in the dawn sector.

The ground and space based observations show signs of early morning drift enhancement as compared to that of the evening hours over the Indian region. Also such enhancement is not seen on other days. Since vertical drifts as obtained from ionosonde can be erroneous due to low electron density in the dawn sector, we run the TIE-GCM model to obtain the vertical plasma drifts and hmF2 in the dawn sector. Please note that the TIE-GCM is a general circulation model that solves full three-dimensional dynamical thermospheric wind equations. The TIE-GCM is a nonlinear, self-consistent 3-D thermospheric–ionospheric model that provides low latitude plasma drifts as one of its outputs. The model uses three dimensional momentum, energy, and continuity equations for different ions, and neutral species. The model uses 5° × 5° latitude and longitude grids as default simulation settings with 29 constant pressure levels in the vertical direction covering to from 97 to 500 km. The model takes F10.7solar flux, high latitude electric potentials from Heelis et al. (1982) or Weimer (2005) as inputs. More details about the model can be found in the Dickinson et al. (1981), Roble et al. (1988), Richmond et al. (1992), and Qian et al. (2014). This model has been widely used for electrodynamic changes during storm time, compositions, and vortex in plasma etc. (e.g., Hagan et al., 2007; Qian et al., 2009).

In this study,we utilized TIE-GCM model run to study this magnetic storm between 09:00 UT and 03:00 UT on December 20–21, 2015 with default resolution of the model which is 5° by 5° latitude and longitudinal (spatial) and 20 min temporal resolution. The Weimer (2005) model inputs used for high latitude potentials. Figures 9a–9c shows the model calculated parameters and virtual height as obtained from the CADI

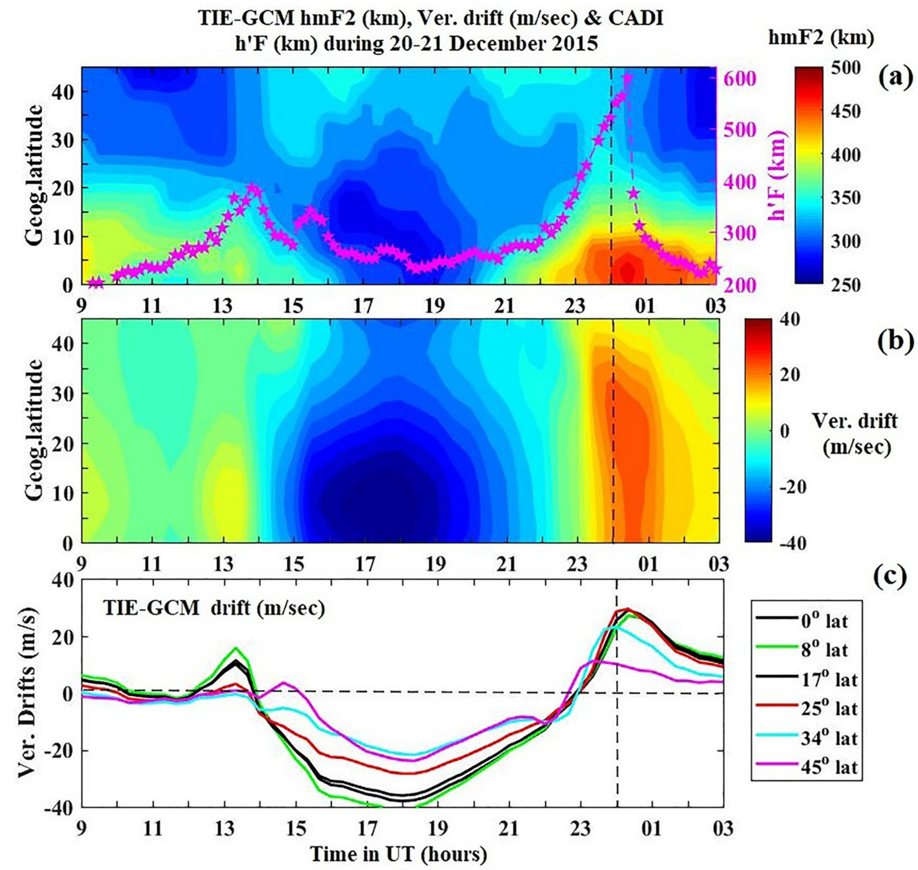

Figure 9. Shows hmF2 (km), h′F (km) and vertical drifts variations over Indian sector (a) hmF2 (color plot) calculated by the thermospheric ionospheric electrodynamics general circulation model (TIE-GCM) and h′F (pink color) obtained from Canadian advanced digital ionosonde (CADI) ionosonde at Tirunelveli (8.73°N, 77.70°E), (b) TIE-GCM vertical plasma drift (m/sec) variations over Indian sector, and (c) TIE-GCM vertical plasma drifts. The hmF2 and vertical plasma drifts calculated at the fixed longitude at ∼77°E and at different latitudes in the northern hemisphere during December 20–21, 2015.

ionosonde over the equatorial station at Tirunelveli. The top panel (a) of the figure shows the variation of the TIE-GCM hmF2 (maximum ionization height) in the km with the latitudes over Indian longitude at ∼77°E. The pink color line plot shows virtual height variations over the Tirunelveli station. From the Figure, we can see clearly that both the model results and observations are showing enhancements in their values during the pre-sunrise hours at 00:00 UT (05:30 IST) at around 8.73°N, 77.70°E. During the evening hours enhancements also observed in the model hmF2 but this enhancement is not as much as ionosonde. The middle panel (b), shows vertical plasma drift variations as calculated by the model over the Indian longitudes. In this panel vertical plasma drift enhancements is noticed upto around 45°N latitudes. The first vertical plasma drift enhanced over the higher latitudes and after some delay over the lower latitudes. The bottom panel (c) of the figure shows latitudinal variations (0°N, 8°N, 17°N, 25°N, 34°N, and 45°N) of the model drifts in the northern hemisphere overthe Indian sector. In the figure, one can see the pre-sunrise hour drift enhancement as compared to the sunset hour drifts. During the pre-sunrise hours also there is delay in ionospheric height enhancement. After post-sunset, the vertical plasma drift oscillations in the model are not as significant as seen in the ionosonde drifts. However, such oscillations can be seen in the model hmF2 which is not shown here.

The DSMP satellite also showed enhanced vertical drifts during this period with similar magnitude and fluctuations in ion density suggesting the presence of irregularities supports our observations. To understand the physical changes in the ionosphere and compare the observed variations in the ionosphere during this space weather event, we run the popular physics based TIE-GCM model.

The vertical plasma drift and hmF2 calculated by the model also showed enhancement during the pre-sunrise hours. However the night time oscillations are not seen in the mode drift. The simultaneous height enhancement during the evening hours and night time oscillations are also observed in the model hmF2 with less magnitudes (not shown here). So, vertical plasma drifts measured by all CADI ionosonde, DMSP satellite and TIE-GCM model show upward enhancement in the dawn sector indicating that the ionosonde measured vertical plasma drifts can be reliable and are not artifacts of the measurements. The magnitude of the CADI vertical plasma drift also matches very well with the satellite observations.

4. Discussions

The important findings from our results as described earlier are: (a) the twin episodes of PRE separated by few 10 s of minutes in the dusk sector over equator where height enhancement/reduction is linked to the undershielding/overshielding conditions respectively which are also simultaneously noticed at other latitudes; (b) the unusual height enhancement in the dawn sector due to strong eastward disturbance dynamo electric field associated with dawn sector electrodynamics that is, peculiar to this storm, (c) the vertical and zonal plasma drifts showing oscillatory behavior throughout the night time with their anticorrelation that are associated with substorm activities at times, (d) the periodogram analysis showing dominant periods in vertical drift, IEFy and AE index at ~30 min and 60 min, (e) cross-wavelet and wavelet coherence analysis on the vertical drifts, IEFy and AE suggesting that ~30 min period as seen in drifts are related to IEFy only; while ~60 min period as seen in the vertical drift could be caused by both IEFy and AE related eastward electric field penetration. Also we noticed EEJ strength fluctuations in the post-midnight sector that is, linked with plasma drift oscillations as seen in the Doppler drift observations.

Now we discuss the causes for storm-time drifts and PRE variations in the pre-midnight hours that deviated from the quiet time behavior. As per the Farley et al. (1986), PRE in zonal electric field in the dusk sector is believed to be produced by E and F region dynamos under quiet-time conditions. The PRE development across the dusk sector has been explained in many articles in the past. Here, we extend it briefly to understand the twin episodes of PRE in the dusk sector. It is driven mostly by eastward zonal neutral winds in the F region when blown perpendicular to magnetic field sets up downward polarization electric field or vertical upward Pedersen current when E regions at conjugate point simultaneously undergo sunset leading to the conductivity gradients across the longitudes. The vertical polarization electric field so developed maps to low latitudes due to equipotential field lines and drives westward Hall currents in the low latitude E region. However, this produces polarization electric field due to presence of conductivity gradient across the E region terminators in the dusk sector. This polarization electric field maps back to F region and causes first upward drift (nightside) and then downward drift (dayside). The same mechanism has been invoked to explain the dawn sector PRE by many (Kelley et al., 2014). However, in this case, eastward neutral wind drives downward polarization electric field which drives westward Hall current. Due to presence of conductivity gradients, this causes accumulation of positive charges across the sunrise terminator which again maps back to the F region as upward drift in the sunrise sector. Since dawn sector is usually considered as switch over time from the F-region dynamo to E region dynamo, it is possible that both E and F region dynamos co-exist simultaneously and can cause complicated electrodynamics in the dawn sector. But during geomagnetic storms, the undershielding/overshielding convection electric fields play significant role in causing modifications in the h′F (km) and hence PRE drifts. Also due to storm-related disturbance dynamo electric fields of eastward/westward polarity can be very strong and opposite to the normal quiet time electric fields. This can cause downward drift in the dusk sector but can cause upward drifts in the dawn sector. The PP electric field occurs in the low latitude region due to sudden change in the polarity of the interplanetary magnetic fields during the magnetic storm (Abdu et al., 1998; Chakrabarty et al., 2006; Kikuchi et al., 1996; Sastri et al., 1992; Sekar & Chakrabarty, 2008). The PP can occur more than one hour due to the changes in magnetic field configuration due the changes in polar cap potential (Basu et al., 2007; Fejer et al., 1990). It is believed that it can penetrate into the low latitude ionosphere without shielding for many hours when the magnetic activity continued to intensify and Bz component remains southward (Huang et al., 2005). We are interested to know the causes for the twin episodes of PRE over the

Tirunelveli at ∼18:30 and 21:00 IST on the December 20, 2015 (shown by the number 1 and 2 respectively in the Figure 2). The wavelet analysis suggested that they could be caused by both AE and IEFy. But wavelet coherence analysis suggested that first rise and then fall of PRE is related possibly to the prompt penetration (undershielding) and overshielding electric fields. Using the ROCSAT-1 satellite data for July 15, 2000 major magnetic storm event, Basu et al. (2001) reported that eastward penetration electric field could be associated with IMF Bz southward turning over South Atlantic region. However, for the same geomagnetic storm of July 15, 2000, Sastri (2002) reported a sudden reduction of F layer height with reference to quiet period over Indian stations at midnight that is, associated with possible westward penetration electric field. This suggests that storm can have different effects at different longitude sectors based on the local time. In a recent report, Ram Singh and Sripathi (2017) have also shown that the virtual height enhancement/reduction could be related to the undershielding/overshielding convection electric fields during the midnight sector over Indian stations. However, for the same storm, the strong eastward penetration of electric field in the European sector caused strong upward plasma drift in the dusk sector to produce strong scintillations (Cherniak & Zakharenkova, 2016).

Next we examine the anti-correlation between zonal and vertical drift oscillations as seen here using basic ideas of storm-time low latitude electrodynamics based on Abdu et al. (1998). Based on this model, the low latitude vertical/zonal drifts could be controlled mainly by (a) Hall conduction, (b) neutral wind dynamo and (c) vertical currents arising from divergence of horizontal (zonal) currents. They suggested that zonal drifts can be driven by a vertical Hall electric field which is induced by primary zonal electric field in the E region and mapped to the F region through field line mapping as field lines are equipotential. They can also cause storm time fluctuations in the zonal drifts (that is anti-correlated to vertical drifts). For this mechanism to operate, significant variation in the ratio of field-line integrated Pedersen conductivity in both E and F region is necessary. As per their model, the anti-correlation of westward zonal drifts with upward vertical drifts can be due to eastward prompt penetration electric fields. It is also possible to modify the PRE electric fields by reducing or increasing the off equatorial E region conductivity. If off-equatorial E region conductivity could be modified as highs and lows as per the E region electron density, it is possible to modify the PRE as lows and highs respectively. But one can ask how enhanced E region electron density is produced in the night? It is believed that particle precipitation during geomagnetic storms can modify the E region conductivity and the twin PRE as seen in this storm could be liked to such conductivity gradients. While South Atlantic Magnetic Anomaly (SAMA) in South America is famous for enhanced E region ionization due to particle precipitation during geomagnetic storms due to weak geomagnetic field, it is not clear whether such enhanced particle precipitation over Indian longitude is also possible and whether they could led to this twin episodes of PRE as there is no such magnetic anomaly over India. Alternately, if zonal winds and wind shears can modify the Es layer and hence E region conductivity, it is also possible to observe such twin PREs during storms. Santos et al. (2016) have investigated zonal and vertical drifts using both observations and simulations and proved that zonal and vertical drifts can arise from competition between zonal neutral winds, Hall conduction and E region conductivity gradients. They suggested that the Pedersen conductivity weighted zonal winds arising from F layer density, Hall and Pedersen field line integrated conductivities and additional ionization in the nighttime E region that modifies the conductivity ratios are believed to play significant roles in the vertical and zonal drift oscillations under forcing by storm time penetration electric fields. It is believed that the zonal plasma drift follows thermospheric zonal winds when E region conductivity is very small. Accordingly, here westward drifts as seen in the present case could be indicative of westward thermospheric winds. But the anti-correlation between vertical and zonal drifts as seen here exists only if the penetrating zonal electric field induces a Hall conduction and by vertical current flow arising from divergence of horizontal currents. The storm-time thermospheric zonal winds at low latitudes become westward and they drive westward plasma drift. However, it is believed that many cases of westward plasma drifts in the post-sunset are unrelated to westward thermospheric winds but can be driven entirely by prompt penetration electric fields. They can drive disturbance zonal drifts into either westward or eastward direction depending upon penetrating zonal electric fields. Since we see oscillating zonal drifts in our present case, we believe that prompt penetrating electric fields dominated the low latitude ionosphere in the pre-midnight sector. Since IMF Bz was in southward direction for several hours for this storm, we believe that in addition to PP electric fields, DD electric fields are also might be playing role in modifying the low latitude ionosphere. Accordingly, the magnetospheric electric fields and disturbance dynamo electric fields are investigated further. The direction of DD electric fields during post-sunset hours is westward which can suppress the PRE during this time. However, we have seen the enhancement of upward drifts in the evening hours which is opposite to the zonal plasma drifts. So, we believe that rather than westward neutral winds that drive thermospheric wind dynamo due to disturbance wind dynamo effect, prompt penetration eastward electric field through their effect of induced vertical Hall electric fields are driving plasma in westward direction. Such effects have been noticed over Brazilian sector. As per the current understanding, if there are no disturbance electric fields due to disturbance wind dynamo effect, usually, eastward penetration (undershielding effect) in the sunset sector leads to increase of the virtual height. But if westward electric field is penetrated (overshielding effect), it leads to reduction of virtual height. However, if the southward turning of the IMF Bz is prolonged for long time like the one we have presented here, it is possible that we may see combination of PP and DD effects simultaneously. So, the double PRE as seen in the present observations in the pre-midnight could be due to the impact of undershielding and overshielding electric fields along with westward DD electric field.

Now we examine why sudden decrease of PRE immediately after first PRE and then again increased during the pre-midnight hours based on periodogram analysis. Earle and Kelley (1987) and Gonzales et al. (1979) have studied the frequency dependent shielding between ionosphere and magnetosphere. They investigated the geomagnetic storm event during 17–18 February 1976 and found the significant dominance of 1.0 h periodicity in the southward component (Bz) of IMF as well as in the electric fields at auroral and dip equatorial stations. On the other hand, Sastri et al. (2000) reported periodicities in the range of 25–35 min in the F region vertical plasma drifts (driven by zonal electric field) during nighttime over dip equator. They suggested that these periods are in coherence with the variations in the Bz component of interplanetary magnetic field as well as with the variations in the substorm activity index namely AE. In our observation, Figure 6 also shows ~20–35 min as a dominant period in IEFy but ~60 min period as a dominant in both IEFy and AE index, which seems to be affecting the F region ionosphere over equatorial latitudes at times. Chakrabarty et al. (2008) also presented simultaneous presence of IEFy and substorm effects on equatorial F layer in the pre-midnight sector. They showed that the variation in virtual height follows the slowly varying component of the AE index and fast fluctuations (~42 min, periods) in the equatorial F layer vertical plasma drift corresponding to the zonal electric field which is mostly controlled by IEFy variations. Using the periodogram and phase spectral analysis, they have explained the distinct effects of IEFy and AE index in the equatorial F layer height. They suggested that the out of phase relationship between drift and IEFy residuals is possibly due to the eastward perturbation electric field (overshielding electric fields), however, in phase relationship between drift and AE is related to substorm activity intensification of auroral electrojet current systems. In our analysis (in Figure 6), we presented the effect of IEFy electric field and substorm driven electric fields on the equatorial F region vertical drift. During the dusk sector, when vertical drift varies between ±~30 m/sec (Figure 5), wavelet analysis show ~30 and ~60 min periods in drift, IEFy and AE index. The wavelet coherence analysis between residual drift and IEFy showed good phase relationship with dominant periods of ~30 and 60 min at ~18:30 and 21:00 ISTon December 20 (Figure 7c), but at the same time ~30 min periods are out of phase with AE. At around 20:00 IST, 30 min periods are out of phase between drift, IEFy and AE, but at the same time, ~60 min period is in same phase with AE but out of phase with IEFy. The periods of ~60 min in vertical drift at ~21:00 IST are in same phase as that of IEFy and AE. So, periods of ~30 min at ~18:30 on December 20 are mainly due to the IEFy. However, ~60 min period between ~20:00 and 23:00 IST is believed to be related to combined effect of both IEFy and AE index. The oscillations as seen in the EEJ strength also suggest that they could be linked to such electric field oscillations.

Now we will explore the causes for anomalous vertical drifts during dawn sector that causes pre-sunrise spread F irregularities. Since virtual height went up to as high as ~600 km during this period, we believe that the plasma irregularities as seen during this period could be generated at the dawn sector only and are unlikely to be related to post-sunset electrodynamics. But this much height rise is a surprise as such rise is not seen during entire month and entire year. So, it is very unique event. To understand this, we have explored several possible mechanisms including the role of winter season. Somayajulu et al. (1991) have investigated the equatorial F layer height and vertical drifts derived using ionosonde during a geomagnetic storm event. In their observations, it is seen that height rise of ~590 km similar to the current event. Their observations showed the possibility of drift velocities reaching as high as ~100 m/s in the dawn sector. Using magnetometer observations from high, mid and low latitudes, they suggested that substorm related electric fields could be responsible for such rise in the drift velocity. Interestingly, it is seen that their observations also correspond to November which is same season as present observations. So, it is possible that ionosphere during winter solstice could be conducive for mapping of electric fields without much attenuation to the equator in dawn sector which ultimately causes the height to rise. Based on San Marco D satellite, Aggson et al. (1995) have reported that enhancement in eastward electric field near the pre-sunrise period do occur in the equatorial F-region. They found that enhancement in zonal electric field appears to correlate seasonally with magnetic field configuration. Nicolls et al. (2006) suggested that it is not necessary that eastward electric field produce an upward enhancement in vertical plasma drift because sometimes upward drifts are enhanced due to decreasing westward electric field in conjunction with sufficient recombination. Anomalous enhancement of eastward zonal electric field in the sunrise sector using San Marco D satellite were found to be similar to evening PRE drifts (Aggson et al., 1995). They suggested that such enhancement is found to be more during winter and low solar activity periods. Since our observations presented here correspond to winter, present results support the above proposed mechanism. Based on C/NOFS drift and ion density observations, Kelley et al. (2014) also suggested that dawn sector increase in vertical drift could be similar to dusk sector electrodynamics. They suggested that polarization electric fields in the dawn sector could be generated under eastward electric field. This can lead to the development of pre-sunrise drifts. During the magnetically quiet and solar minimum conditions, Zhang et al. (2015) have reported a statistical study of occurrence of equatorial ionospheric vertical plasma drift enhancement near sunrise period using ROCSAT-1 observations. They suggested that enhancement in vertical plasma drift near sunrise period is most frequent in June solstice and least frequent in December solstice. They also said it may depend on the magnetic declination. Zhang et al. (2016) later showed using ground based digisonde over Jicamarca that sunrise vertical drift enhancement can lift the F2 layer peak to very high altitude which can ultimately be seen as F_3 layers in the topside and the F2 layer peak density tend to decrease as compared to days having no such pre-sunrise enhancements. However, we didn't see any F_3 layers during this period. It may be mentioned that we also examined the ion density and ion vertical drifts as measured by in situ DMSP satellite at ~850 km altitude in the dawn sector over

India on December 20–21, 2015 to re-confirm that what we observe in ionosonde drifts in the dawn sector is indeed accurate and reliable. The DSMP satellite measurements also showed enhanced vertical drifts during this period with near similar magnitude and fluctuations in ion density suggesting presence of irregularities supports that our observations are reliable.

Under the geomagnetic disturbed conditions, Reddy et al. (1990) presented role of magnetospheric substorm related disturbance electric fields over the mid and low latitude ionosphere. They suggested that enhancement in virtual height (h′F) of F layer during post-midnight to morning hours could be affected by two possibilities. One possibility is through the generation of large secondary electric fields at auroral latitudes. They suggested that whenever such large secondary electric fields are generated in the ionosphere at auroral and subauroral latitudes during substorms which are higher than externally imposed primary convection electric fields, they can affect the equatorial electrodynamics in the dawn sector. The second possibility could be that secondary polarization electric field may be generated in the inner magnetosphere on the nightside during substorm due to impulsive injection and spatially non uniform drift motion of energetic ions. Under these conditions, it is possible that secondary polarization electric field can affect the equatorial ionosphere and can push the F layer to very higher altitudes. Since we don't see good correlation of drifts with IEFy, it is possible that secondary electric fields might play dominant role than externally imposed magnetospheric electric fields leading to the drift enhancement in the dawn sector. Sastri et al. (1997) have made a comparative study under a geomagnetic storm using simultaneous Kodaikanal and Fortaleza vertical drifts along with H and D components of asymmetric ring current (ASY-H and ASY-D) to suggest that electric field polarity gets opposite in nature during growth and recovery phases of ring current intensification which manifest as westward and eastward electric field. Accordingly, the results suggest that virtual height (h′F) enhancement near pre sunrise periods at ~05:30 IST could be related to effect of substorm driven polarization electric field and eastward DD electric fields that are linked with unique dawn sector electrodynamics due to this storm process as all the stations showed enhancement simultaneously.

5. Summary

We have presented the storm-time electrodynamics of the equatorial and low latitude ionosphere in the nighttime due to long lasting geomagnetic storm event of December 19–21, 2015 using chain of ionosonde observations from equator to low latitude stations. We observed large variations in density, in the vertical/zonal drifts as well as height oscillations throughout the night in response to storm time modifications in the electrodynamics. Also we observed anticorrelation between vertical and zonal drifts as reported in Brazilian sector. Accordingly the role of vertical polarization electric field due to prompt penetration zonal electric fields in causing the anti-correlation of zonal and vertical drifts is discussed. In addition, we also discussed several other possibilities for the drift oscillations. We performed wavelet, cross wavelet and wavelet coherence analysis using interplanetary, geomagnetic and ionospheric data to identify the sources for these oscillations. From this analysis, the following important points emerge: (a) good association of twin episodes of PRE between at ~18:00 and 22:00 IST is identified with undershielding and overshielding electric fields respectively, (b) the results suggest that height increase of upto ~600 km in the dawn sector and subsequent occurrence of plasma irregularities could be due to strong eastward disturbance dynamo electric field fluctuations linked with peculiar electrodynamics in the dawn sector, (c) the vertical and zonal drift oscillations in the pre-midnight on December 20 could be due to the combined storm-substorm effects, (d) the cross wavelet analysis suggest that equatorial plasma drifts are correlated mainly with IEFy at shorter periods (<30 min) but longer (~60 min) periods are correlated with IEFy and AE activity at intervals. The wavelet coherence analysis also suggests that such relations do exists with high coherence. So, the important conclusion that emerges from this study is that it is difficult to distinguish the PP and DD electric field effects if both are present simultaneously using cross wavelets; however, it is possible to distinguish the effect of IEFy and AE to some extent using wavelet coherence analysis. (e) the satellite observations and model (TIE-GCM) analysis near the dawn sector further confirms that vertical plasma drift enhancements could be affected by the storm induced disturbance dynamo electric fields.

Data Availability Statement

Solar wind and geomagnetic indices data are available from the NASA CDAWeb (http://cdaweb.gsfc.nasa.gov.), and World Data Center (WDC), Kyoto University, Japan (http://wdc.kugi.kyoto-u.ac.jp). The complete outputs of TIE-GCM simulations for December 19–21, 2015 storm are available in the public of the Community Coordinated Modeling Center website (https://ccmc.gsfc.nasa.gov). The CADI ionosonde data presented in this paper can be accessed at http://doi.org/10.5281/zenodo.5087361.

Acknowledgments

The research work presented here is made possible through the funding support from IIG, DST, Govt. of India, Navi Mumbai. The authors wish to thank the Director, IIG for his support and also providing access to EEJ data. SS would like to thank the ICTP, Trieste, Italy for its support under its associateship program. We wish to thank Mr. Emperumal and Mr. SelvaRaj, technical officers at EGRL at Tirunelveli and Mr. P Tiwari, technical officer at KSK-GRL, Allahabad for maintaining and operating the CADI ionosondes at Tirunelveli/Allahabad. We also would like to thank Mr. Buduru Suneel Kumar, Scientist-in-charge, TIFR Balloon Launch Facility, Hyderabad for providing CADI data at Hyderabad. We thank the staff of CCMC for their patience and cooperation on troubleshooting, crashed runs for the model.

References

Abdu, M. A., Bittencourt, J. A., & Batista, I. S. (1981). Magnetic declination control of the equatorial F region dynamo electric field development and spread F. *Journal of Geophysical Research*, *86*, 11443–11446. https://doi.org/10.1029/ja086ia13p11443

Abdu, M. A., Jayachandran, P. T., MacDougall, J., Cecile, J. F., & Sobral, J. H. A. (1998). Equatorial F region zonal plasma irregularity drifts under magnetospheric disturbances. *Geophysical Research Letters*, *25*(22), 4137–4140. https://doi.org/10.1029/1998gl900117

Abdu, M. A., MacDougall, J., Batista, I. S., Sobral, J. H. A., Jayachandran, P. T. (2003). Equatorial evening pre reversal electric field enhancement and sporadic E-layer disruption: A manifestation of E and F-region coupling. *Journal of Geophysical Research*, *108*(A6), 1254. https://doi.org/10.1029/2002JA009285

Aggson, T. L., Herrero, F. A., Johnson, J. A., Pfaff, R. F., Lmkso, H., Maynardt, N. C., & Moses, J. J. (1995). Satellite observations of zonal electric fields near sunrise in the equatorial ionosphere. *Journal of Atmospheric and Terrestrial Physics*, *57*, 19–24. https://doi.org/10.1016/0021-9169(93)e0013-y

Araki, T., Allen, J. H., & Araki, Y. (1985). Extension of a polar ionospheric current to the night side equator. *Planetary and Space Science*, *33*(1), 11–16. https://doi.org/10.1016/0032-0633(85)90137-0

Astafyeva, E., Zakharenkova, I., Hozumi, K., Alken, P., Coïsson, P., Hairston, M. R., & Coley, W. R. (2018). Study of the equatorial and low-latitude electrodynamic and ionospheric disturbances during the 22–23 June 2015 geomagnetic storm using ground-based and space borne techniques. *Journal of Geophysical Research: Space Physics*, *123*, 2424–2440. https://doi.org/10.1002/2017ja024981

Basu, S., Basu, S., Groves, K. M., Yeh, H. C., Su, S. Y., Rich, F. J., et al. (2001). Response of the equatorial ionosphere in the South Atlantic Region to the Great Magnetic Storm of July 15, 2000. *Geophysical Research Letters*, *28*, 3577–3580. https://doi.org/10.1029/2001gl013259

Basu, S., Basu, S., Rich, F. J., Groves, K. M., MacKenzie, E., Coker, C., et al. (2007). Response of the equatorial ionosphere at dusk to penetration electric fields during intense geomagnetic storms. *Journal of Geophysical Research*, *112*, A08308. https://doi.org/10.1029/2006JA012192

Blanc, M., & Richmond, A. D. (1980). The ionospheric disturbances dynamo. *Journal of Geophysical Research*, *85*, 1669. https://doi.org/10.1029/ja085ia04p01669

Chakrabarty, D., Sekar, R., Narayanan, R., Patra, A. K., & Devasia, C. V. (2006). Effects of interplanetary electric field on the development of an equatorial spread F event. *Journal of Geophysical Research*, *111*, A12316. https://doi.org/10.1029/2006JA011884

Chakrabarty, D., Sekar, R., Sastri, J. H., & Ravindran, S. (2008). Distinctive effects of interplanetary electric field and substorm on nighttime equatorial F layer: A case study. *Geophysical Research Letters*, *35*, L19108. https://doi.org/10.1029/2008GL035415

Cherniak, I., & Zakharenkova, I. (2016). First observations of super plasma bubbles in Europe. *Geophysical Research Letters*, *43*, 11137–11145. https://doi.org/10.1002/2016GL071421

Dickinson, R. E., Ridley, E. C., & Roble, R. G. (1981). A three-dimensional general circulation model of the thermosphere. *Journal of Geophysical Research*, *86*(A3), 1499–1512. https://doi.org/10.1029/JA086iA03p01499

Earle, G. D., & Kelley, M. C. (1987). Spectral studies of the sources of ionospheric electric fields. *Journal of Geophysical Research*, *92*, 213. https://doi.org/10.1029/ja092ia01p00213

Farley, D. T., Bonelli, E., Fejer, B. G., & Larsen, M. F. (1986). The pre reversal enhancement of the zonal electric field in the equatorial ionosphere. *Journal of Geophysical Research*, *91*, 13723–13728. https://doi.org/10.1029/ja091ia12p13723

Fejer, B. G., de Paula, E. R., Gonzalez, S. A., & Woodman, R. F. (1991). Average vertical and zonal F region plasma drifts over Jicamarca. *Journal of Geophysical Research*, *96*(A8), 13901–13906. https://doi.org/10.1029/91JA01171

Fejer, B. G., Larsen, M. F., & Farley, D. T. (1983). Equatorial disturbance dynamo electric fields. *Geophysical Research Letters*, *10*(No.7), 537–540. https://doi.org/10.1029/gl010i007p00537

Fejer, B. G., Scherliess, L., & de Paula, E. R. (1999). Effects of the vertical plasma drift velocity on the generation and evolution of equatorial spread. *Journal of Geophysical Research*, *104*, 19859–19869. https://doi.org/10.1029/1999ja900271

Fejer, B. G., Spiro, R. W., Wolf, R. A., & Foster, J. C. (1990). Latitudinal variation of perturbation electric fields during magnetically disturbed periods: 1986 SUNDIAL observations and model results. *Annals of Geophysics*, *8*, 441–454.

Gonzales, C. A., Kelley, M. C., Fejer, B. G., Vickrey, J. F., & Woodman, R. F. (1979). Equatorial electric fields during magnetically disturbed conditions: 2. Implications of simultaneous auroral and equatorial measurements. *Journal of Geophysical Research*, *84*, 5803. https://doi.org/10.1029/ja084ia10p05803

Hagan, M. E., Maute, A., Roble, R. G., Richmond, A. D., Immel, T. J., & England, S. L. (2007). Connections between deep tropical clouds and the Earth's ionosphere. *Geophysical Research Letters*, *34*, L20109. https://doi.org/10.1029/2007GL030142

Heelis, R. A., Kendall, P. C., Moffett, R. J., Windle, D. W., & Rishbeth, H. (1974). Electrical coupling of the E- and F-regions and its effects on the F region drifts and winds. *Planetary and Space Science*, *22*, 743–756. https://doi.org/10.1016/0032-0633(74)90144-5

Heelis, R. A., Lowell, J. K., & Spiro, R. W. (1982). A model of the high-latitude ionospheric convection pattern. *Journal of Geophysical Research*, *87*(A8), 6339–6345. https://doi.org/10.1029/JA087iA08p06339

Huang, C. S., Foster, J. C., & Kelley, M. C. (2005). Long duration penetration of the planetary electric field to the low altitude ionosphere during the main phase of magnetic storms. *Journal of Geophysical Research*, *110*, A11309. https://doi.org/10.1029/2005JA011202

Huang, C. S., Sazykin, S., Chau, J. L., Maruyama, N., & Kelley, M. C. (2007). Penetration electric fields: Efficiency and characteristic time scale. *Journal of Atmospheric and Solar: Terrestrial Physics*, *69*(10–11), 1135–1146. https://doi.org/10.1016/j.jastp.2006.08.06

Kamide, Y., & Chian, A. C.-L. (2007). *Handbook of the solar-terrestrial environment* (p. 10). Berlin: Springer.

Kelley, M. C., Fejer, B. G., & Gonzales, C. A. (1979). An explanation for anomalous equatorial ionospheric electric fields associated with a northward turning of the interplanetary magnetic field. *Geophysical Research Letters*, *6*, 301–304. https://doi.org/10.1029/GL006i004p00301

Kelley, M. C., Makela, J. J., Chau, J. L., & Nicolls, M. J. (2003). Penetration of the solar wind electric field into the magnetosphere/ionosphere system. *Geophysical Research Letters*, *30*(4), 1158. https://doi.org/10.1029/2002gl016321

Kelley, M. C., Rodrigues, F. S., Pfaff, R. F., & Klenzing, J. (2014). Observations of the generation of eastward equatorial electric fields near dawn. *Annals of Geophysics*, *32*, 1169–1175. https://doi.org/10.5194/angeo-32-1169-2014

Kikuchi, T. (1986). Evidence of transmission of polar electric fields to the low latitude at times of geomagnetic sudden commencements. *Journal of Geophysical Research*, *91*(A3), 3101–3105. https://doi.org/10.1029/JA091iA03p03101

Kikuchi, T., Lühr, H., Kitamura, T., Saka, O., & Schlegel, K. (1996). Direct penetration of the polar electric field to the equator during a DP 2 event as detected by the auroral and equatorial magnetometer chains and the EISCAT radar. *Journal of Geophysical Research*, *101*(A8), 17161–17173. https://doi.org/10.1029/96JA01299

Liu, J., Liu, L., Nakamura, T., Zhao, B., Ning, B., & Yoshikawa, A. (2014). A case study of ionospheric storm effects during long-lasting southward IMF Bz-driven geomagnetic storm. *Journal of Geophysical Research: Space Physics*, *19*, 7716–7731. https://doi.org/10.1002/2014ja020273

Marques de Souza, A., Echer, E., Bolzan, M. J. A., & Hajra, R. (2018). Cross-correlation and cross-wavelet analyses of the solar wind IMF B_z and auroral electrojet index AE coupling during HILDCAAs. *Annals of Geophysics*, *36*, 205–211. https://doi.org/10.5194/angeo-36-205-2018

Nicolls, M. J., Kelley, M. C., Vlasov, M. N., Sahai, Y., Chau, J. L., Hysell, D. L., et al. (2006). Observation and Modeling of post-midnight near the magnetic equator. *Annals of Geophysics*, *24*, 1317–1331. https://doi.org/10.5194/angeo-24-1317-2006

Prabhakaran Nayar, S. R., Mathew, T. J., Sreehari, C. V., Sumod, S. G., Devasia, C. V., Ravindran, S., et al. (2009). Electrodynamics of the equatorial F-region ionosphere during pre-sunrise period. *Annals of Geophysics*, *27*, 107–111. https://doi.org/10.5194/angeo-27-107-2009

Qian, L., Burns, A. G., Emery, B. A., Foster, B., Lu, G., Maute, A., et al. (2014). The NCAR TIE-GCM. In J. Huba, R. Schunk, & G. Khazanov (Eds.), *Modeling the ionosphere–thermosphere system* (pp. 73–83). https://doi.org/10.1002/9781118704417.ch7

Qian, L., Solomon, S. C., & Kane, T. J. (2009). Seasonal variation of thermospheric density and composition. *Journal of Geophysical Research*, *114*, A01312. https://doi.org/10.1029/2008JA013643

Ram Singh, & Sripathi, S. (2017). Ionospheric response to 22–23 June 2015 storm as investigated using ground-based ionosondes and GPS receivers over India. *Journal of Geophysical Research: Space Physics*, *122*, 645–711. https://doi.org/10.1002/2017JA024460

Ram Singh, Sripathi, S., Sreeba Sreekumar, Banola, S., Emperumal, K., Tiwari, P., & Suneel Kumar, B. (2015). Low-latitude ionosphere response to super geomagnetic storm of 17/18 March 2015: Results from a chain of ground based observations over Indian sector. *Journal of Geophysical Research: Space Physics*, *120*, 10864–10882. https://doi.org/10.1002/2015ja021509

Rastogi, R. G., & Klobuchar, J. A. (1990). Ionospheric electron content within the equatorial F2 layer anomaly belt. *Journal of Geophysical Research*, *95*(A11), 19045–19052. https://doi.org/10.1029/JA095iA11p19045

Reddy, C. A., Nishida, A., Fukao, S., & Somayajulu, V. V. (1990). Magnetospheric substorm-related electric fields in the ionosphere: Discrepancy of an observation with model prediction. *Geophysical Research Letters*, *17*(12), 2333–2336. https://doi.org/10.1029/gl017i013p02333

Reddy, C. A., Somayajulu, V. V., & Devasia, C. V. (1979). Global scale electrodynamic coupling of the auroral and equatorial dynamo regions. *Journal of Atmospheric and Terrestrial Physics*, *41*, 189–201. https://doi.org/10.1016/0021-9169(79)90012-6

Richmond, A. D., Ridley, E. C., & Roble, R. G. (1992). A thermosphere/ionosphere general circulation model with coupled electrodynamics. *Geophysical Research Letters*, *19*(6), 601–604. https://doi.org/10.1029/92GL00401

Rishbeth, H. (1971). Polarization fields produced by winds in the equatorial F-region. *Planetary and Space Science*, *19*, 357–369.

Roble, R. G., Ridley, E. C., Richmond, A. D., & Dickinson, R. E. (1988). A coupled thermosphere/ionosphere general circulation model. *Geophysical Research Letters*, *15*(12), 1325–1328. https://doi.org/10.1029/GL015i012p01325

Santos, A. M., Abdu, M. A., Souza, J. R., Sobral, J. H. A., & Batista, I. S. (2016). Disturbance zonal and vertical plasma drifts in the Peruvian sector during solar minimum phases. *Journal of Geophysical Research: Space Physics*, *121*, 2503–2521. https://doi.org/10.1002/2015JA022146

Sastri, J. H. (1988). Equatorial electric fields of ionospheric disturbance dynamo origin. *Annals of Geophysics*, *6*, 635–642.

Sastri, J. H. (2002). Equatorial geomagnetic and ionospheric effects of substorms. *Indian Journal of Radio and Space Physics*, *31*, 309.

Sastri, J. H., Abdu, M. A., & Sobral, J. H. A. (1997). Response of equatorial ionosphere to episodes of asymmetric ring current activity. *Annales Geophysicae*, *15*(10), 1316–1323. https://doi.org/10.1007/s00585-997-1316-3

Sastri, J. H., Jyoti, N., Somayajulu, V. V., Chandra, H., & Devasia, C. V. (2000). Ionospheric storm of early November 1993 in the Indian equatorial region. *Journal of Geophysical Research*, *105*, 18443–18455. https://doi.org/10.1029/1999JA000372

Sastri, J. H., Ramesh, K. B., & Karunakaran, D. (1992). On the nature of substorm-related transient electric field disturbances in the equatorial ionosphere. *Planetary and Space Science*, *40*, 95–103. https://doi.org/10.1016/0032-0633(92)90152-e

Savitzky, A., & Golay, M. J. E. (1964). Smoothing and differentiation of data by simplified least squares procedures. *Analytical Chemistry*, *36*, 1627–1639. https://doi.org/10.1021/ac60214a047

Sekar, R., & Chakrabarty, D. (2008). Role of overshielding electric field on the development of pre-midnight plume event: Simulation results. *Journal of Atmospheric and Terrestrial Physics*, *70*(17), 2212–2221. https://doi.org/10.1016/j.jastp.2008.04.015

Sekar, R., & Kelley, M. C. (1998). On the combined effects of vertical shear and zonal electric field patterns on nonlinear equatorial spread F evolution. *Journal of Geophysical Research*, *103*, 20735. https://doi.org/10.1029/98ja01561

Somayajulu, V. V., Murthy, B. V. K., & Subbarao, K. S. V. (1991). Response of night-time equatorial F-region to magnetic disturbances. *Journal of Atmospheric and Terrestrial Physics*, *53*(10), 965–976. https://doi.org/10.1016/0021-9169(91)90008-u

Spiro, R. W., Wolf, R. A., & Fejer, B. G. (1988). Penetration of high-latitude-electric-field effects to low latitudes during SUNDIAL 1984. *Annals of Geophysics*, *6*, 39–50.

Torrence, C., & Compo, G. P. (1998). A practical guide to wavelet analysis. *Bulletin of the American Meteorological Society*, *79*, 61–78. https://doi.org/10.1175/1520-0477(1998)079<0061:apgtwa>2.0.co;2

Weimer, D. R. (2005). Improved ionospheric electrodynamic models and application to calculating joule heating rates. *Journal of Geophysical Research*, *110*, A05306. https://doi.org/10.1029/2004JA010884

Zhang, R., Liu, L., Chen, Y., & Le, H. (2015). The dawn enhancement of the equatorial ionospheric vertical plasma drift. *Journal of Geophysical Research: Space Physics*, *120*, 10688–10697. https://doi.org/10.1002/2015JA021972

Zhang, R., Liu, L., Le, H., & Chen, Y. (2016). Evidence and effects of the sunrise enhancement of the equatorial vertical plasma drift in the F region ionosphere. *Journal Geophysical Research: Space Physics*, *121*, 4826–4834. https://doi.org/10.1002/2016JA022491